Journal of the European Ceramic Society 18 (1998) 2307–2312

PII: S0955-2219(98)00236-2
0955-2219/99/$—see front matter

Modelling of the Oxidation Kinetics of a Yttria-doped Hot-pressed Silicon Nitride

F. A. Costa Oliveira†, D. J. Baxter* and J. Ungeheuer

European Commission — DG Joint Research Centre, Institute for Advanced Materials, PO Box 2, NL-1755 ZG Petten, The Netherlands

Abstract

Oxidation kinetics provide essential baseline information on the performance of silicon-based ceramics for high temperature structural applications. A study of the oxidation kinetics of a hot-pressed Si_3N_4 densified with 9 wt% Y_2O_3 was carried out by thermogravimetry in 'dry' synthetic air over the temperature range 800 to 1200°C for 50 h. Data obtained clearly show that oxidation kinetics are mostly non-parabolic suggesting that the oxidation mechanism is more complex than simple diffusion. At 800°C, the kinetics are approximately parabolic, but a linear contribution to the process possibly indicates that the oxidation product is non-protective, allowing internal oxidation to occur. In the temperature range 900 to 1200°C, kinetics are better described by an arctan model suggesting that either SiO_2 devitrification or nitrogen bubble formation reduce the cross-sectional area for diffusion. © *1999 Elsevier Science Limited. All rights reserved*

1 Introduction

The oxidation resistance of silicon nitride-based ceramics derives from a chemically very stable covalent crystal structure combined with the formation of a silicon dioxide (SiO_2) surface layer which acts as a barrier for oxygen diffusion. In the case of the oxidation of polyphase hot-pressed Si_3N_4 materials it is generally difficult to establish the rate controlling mechanism, since the oxidation rate is critically dependent on several parameters, e.g. temperature and time, and oxidation usually involves the formation of complex layers whose properties (e.g. composition, viscosity, degree of crystallinity) change with time thus affecting the overall process.

Although the use of Y_2O_3 produces significantly improved mechanical properties at high temperatures (>1300°C) compared with MgO-doped hot-pressed materials,[1] some compositions of silicon nitride hot-pressed with yttrium oxide are prone to fail catastrophically at temperatures in the range 900–1200°C in oxidising environments.[2–4] This is believed to be due to the fact that at these temperatures, the surface of the material is not completely covered by a protective SiO_2 layer. Thus, the unstable quaternary crystalline phases formed on sintering, which form intergranular phases upon cooling, can readily oxidise, resulting in substantial increases in molar volume.[5,6] This volume change can lead to extensive cracking and rapid degradation of the material at lower temperatures. At higher temperatures (>1200°C), however, this problem is not observed, probably due to the softening of both the oxide layer and the intergranular phase allowing them to deform more easily to relieve oxidation-induced local stresses. It is therefore evident that the nature and content of the intergranular phases play an important role in determining the oxidation resistance of polyphase silicon nitride ceramics.

The goal of this work was to evaluate the influence of temperature on the oxidation kinetics and to establish the role of the intergranular phase in the formation of the oxide layers in order to gain a better understanding of the rate-controlling mechanisms responsible for the degradation of this material in oxidising environments at high temperatures. Various mathematical models were used to fit the weight change data. The fitting was performed mainly as an analytical tool in order to

*To whom correspondence should be addressed. Fax: +31-224-563841; e-mail; baxter@jrc.nl

On leave from INETI, Instituto Nacional de Engenharia e Technologia Industrial, Estrada do Paşo do Lumiar, 1699 Lisboa Codex, Portugal.

provide an understanding of the oxidation mechanism. With mathematical models, however, it has to be accepted that a simple direct correlation between components used in the model and the actual physical causes of observed behaviour may not be clearly definable. This paper highlights the results of an investigation of oxidation behaviour of an yttria-doped silicon nitride and shows the importance of relying on microstructural evaluation in order to assess the reliability of mathematical models fitted to oxidation rate.

2 Experimental

2.1 The material

The material used in this work was Ceranox NH209 (ex Feldmühle AG, Germany) densified by hot pressing at 1750°C under a pressure of 40 MPa using 9·0 wt% Y_2O_3 and 1·7 wt% Fe_2O_3 to a bulk density of 3·33 Mg. m^{-3} and 2% open porosity. The microstructure of the material was studied by means of transmission electron microscopy (TEM) and X-ray diffraction analysis (XRD). Test bars were diamond cut to 3 by 4 mm by 15 mm in size and ground on all faces to a surface roughness of 0·2 μm (R_a).

2.2 Oxidation testing and evaluation

Prior to testing, the dimensions of the samples were measured (accuracy of $\pm 0{\cdot}01$ mm). The samples were ultrasonically cleaned in ethanol for 30 min, dried in a desiccator for at least 10 h and finally weighed (accuracy of $\pm 10\,\mu$g).

Oxidation kinetics were assessed by continuous thermogravimetry over 50 h using an automatic Cahn thermobalance (model Cahn 171, Cahn Instruments Inc., USA) with a sensitivity of $\pm 1\,\mu$g in the 1 g weight change range over the temperature range 800 to 1200°C. The specimens were placed on high purity (> 99·9%) aluminium oxide discs (at 800 and 900°C) and on a Pt wire cage (above 900°C) in an Al_2O_3 crucible suspended from the balance by a 0·5 mm diameter sapphire rod and held in the hot zone of a pure recrystallised alumina furnace tube. Heating was at a fixed rate of 40°C min^{-1}, in flowing 'dry' synthetic air (< 5 ppm H_2O) at a rate of 3 l h^{-1} and a pressure of 0·11 MPa. Weight changes were gathered every 30 s. The correction for the effects of heating, cooling and Pt evaporation (e.g. about 12 μg h^{-1} at 1200°C) was done by subtracting the data obtained in blank experiments carried out prior to each test. Bulk identification of the corrosion products was carried out by XRD and scanning electron microscopy (SEM).

3 Results and Discussion

3.1 Microstructure

The microstructure of the material has been found by X-ray diffraction (XRD) to consist primarily of prismatic hexagonal grains of β-Si_3N_4 surrounded by a crystalline phase identified as $Y_{10}(SiO_4)_6N_2$ (also known as H-phase). By means of electron microdiffraction analysis in a TEM some pockets of $YNSiO_2$ (known as K-phase) as well as $FeSi_2$ inclusions (Fig. 1) were also found. The volume fraction of intergranular phase present was estimated to be $15 \pm 1\%$ (based on 10 images) using image analysis on SEM images from polished cross sections.

3.2 Oxidation behaviour

Isothermal data for the oxidation of Ceranox NH209 in 'dry' air are shown in Fig. 2. It should be noted that these figures only display weight change data at the isothermal temperatures. All data recorded during heating and cooling have not been considered. All curves above 800°C show an offset from the origin due to weight increases on heating. The total weight change recorded at each temperature

Fig. 1. TEM micrograph of Ceranox NH209 showing a $FeSi_2$ inclusion.

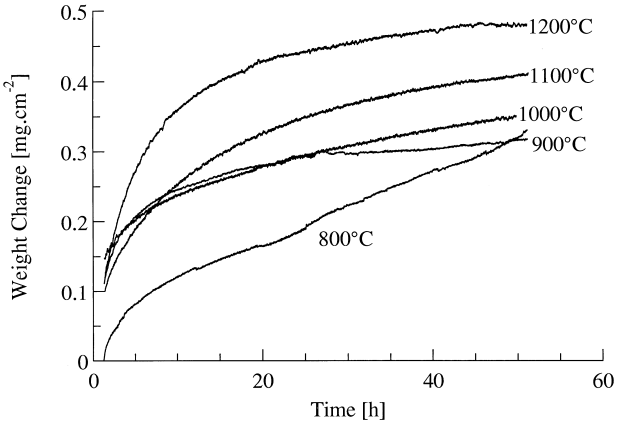

Fig. 2. Oxidation kinetics of Ceranox NH209 at temperatures in the range 800–1200°C.

has been corrected to match the weight change of the sample obtained using an external balance at room temperature. In order to evaluate the kinetics of oxidation of Ceranox NH209 through mathematical fitting, the assumption has been made that at $t=0$ (corresponding to the beginning of the isotherm) the weight change should be zero.

The mechanism of oxidation of Ceranox NH209 is complex and depends critically on temperature which has a significant effect on both the composition and morphology of the silicon dioxide-rich surface layer formed. Plotting the data in Fig. 2, in a logarithmic scale it can be seen that oxidation kinetics, although initially parabolic, change to non-parabolic. This suggests that the oxidation mechanism is more complex than simple diffusion through a single layer surface scale (Fig. 3).

3.3 Oxidation modelling

At 800°C, the kinetics approximate a parabolic law over the period of exposure from approximately 4 to 25 h (Fig. 3). At longer exposure times, however, a linear contribution probably indicates that the oxidation product loses some of its protection, allowing internal oxidation to occur. Figure 4 shows that the surface of the sample exposed at 800°C is porous and cracked in some places. These pores probably result mainly from decomposition of O-apatite which releases nitrogen. Under certain conditions, bubble formation (resulting from the very low solubility of nitrogen in glasses[2]) can lead to disruption of the oxide layer, provided that the nitrogen pressure is sufficiently high to cause the bubble to burst at the material's surface. This may also result in cracking of the oxide layer (as seen in Fig. 4) and thus provide a path that allows gaseous oxygen to flow into the interface between the oxide layer and the unoxidised material. Thus a change from a diffusion-controlled process to an interfacial reaction controlled process should be anticipated for at least a fraction of the surface area of the test piece. Lange *et al.*[2] showed that the quaternary compounds formed within the Si_3N_4–Y_2O_3–SiO_2 system readily oxidise when exposed to oxidising environments at high temperatures. Moreover, oxidation kinetics obtained for one of these phases (i.e. $Si_3Y_2O_3N_4$) were found to be linear due to cracking of the material caused by large volume changes on oxidation. Such cracks can provide preferential paths for oxygen transport giving the enhanced oxidation rate observed in this work. Thus the possibility exists that the overall oxidation rate at 800°C is likely to be influenced by a combination of a diffusion processes and interface reactions; with the contribution by diffusion being dominant. This reasoning may explain the relatively low oxidation resistance (expressed as weight change) at 800°C. The other quaternary phases are also readily oxidised when exposed to air at 1000°C and the observed products of oxidation suggest the following reactions:

$$2YSiO_2N(\text{K phase}) + 1{\cdot}5\,O_2 \rightarrow Y_2Si_2O_7 + N_2 \quad (1)$$

$$Y_{10}(SiO_4)_6N_2(\text{H phase}) + 1{\cdot}5\,O_2 \quad Y_2Si_2O_7 + 4Y_2SiO_5 + N_2 \quad (2)$$

It has been shown[7] that the oxidation mechanism of the H-phase (major intergranular phase present

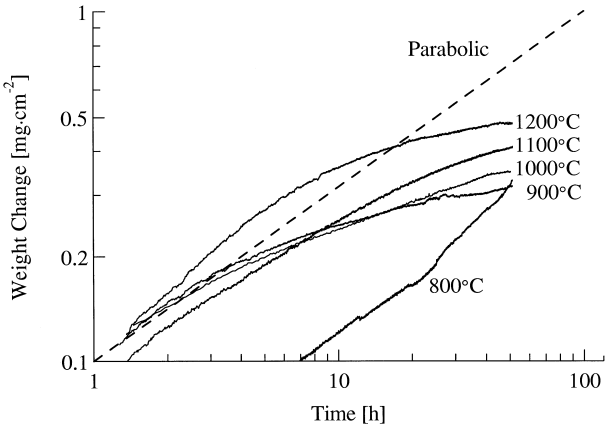

Fig. 3. Logarithmic plot showing of the oxidation kinetics of Ceranox NH209 at temperatures in the range 800–1200°C.

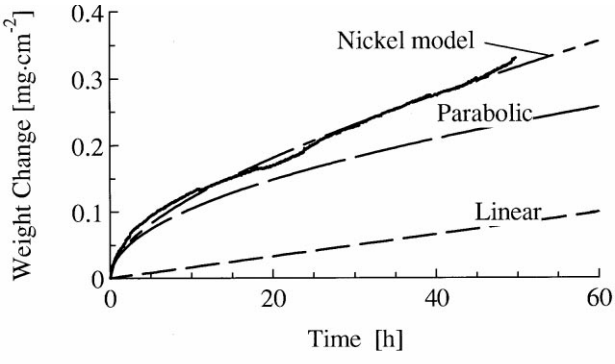

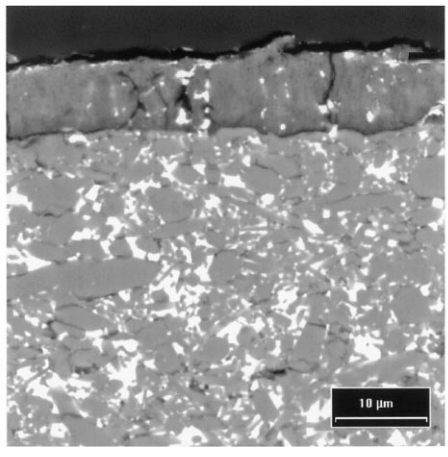

Fig. 4. Fitting of the kinetic data obtained at 800°C and BSE micrograph of a cross-section obtained after 50 h of exposure. (Note that in all micrographs the surface oxide film is shown at the top part of the images.)

in the material under investigation) is complex and involves the formation of intermediate products such as $Y_{4.67}(SiO_4)_3O$ (as evidenced by XRD at temperatures above 900°C), via the oxidation of Y–N apatite to Y–O apatite, followed by further oxidation to $Y_2Si_2O_7$ accompanied by the release of nitrogen. The strongly parabolic character of the oxidation kinetics at 800°C corroborates the finding by Veyret[7] that oxygen uptake through gaseous diffusion is likely to be the slowest process and therefore the rate-controlling step. This would explain why approximately parabolic kinetics were observed. It should be note that some cracks were observed in the bulk material (as seen in Fig. 4). It is not clear, however, whether the cracks were caused by oxidation of the intergranular phase, which induces superficial microcracks as a result of volume changes and/or N_2 release, or are due to cracking on cooling or to damage caused by polishing.

In the temperature range 900 to 1200°C, kinetics are well described by the model developed by Persson *et al.*,[4] over the entire exposure time used, as

$$x = \mathrm{a}\arctan\sqrt{bt} + \mathrm{c}\sqrt{t} + \mathrm{d} \qquad (3)$$

although at 1000°C the multiple law model proposed by Nickel[8] can also be applied (Fig. 5)

$$x = k_{\mathrm{lin}}t + k_p\sqrt{t} + k_{\log}\log t \qquad (4)$$

where the mass change per unit area x is expressed as a function of time t by several constants, i.e. a, b, c and d and the linear (k_{lin}) , parabolic (k_p) and logarithmic ($k_{\log}$) rate constants.

The arctan component of eqn (3) is derived by incorporation of a function $A(t)$ in the parabolic rate law ($x^2 = K_{\mathrm{p}}\mathrm{t} + \mathrm{const.}$, where $x = \Delta m/A$), which describes the decrease of the cross-section area of the amorphous phase available for oxygen diffusion. This model is based on the assumption that the oxygen diffusion through the crystalline phase is negligible compared to that through the amorphous phase. For eqn (4), the linear component would represent surface reactions, the parabolic component would reflect diffusion control and the logarithmic component would describe the effect of progressively decreasing surface area (i.e. due to crystallisation of glassy SiO_2). Diffusion could be of either additive/impurities or oxygen/nitrogen through the surface oxide layer.

Deviations from non-parabolic behaviour can be attributed to crystallisation of the oxidation layer since the effective surface area, through which the oxidant can attack is reduced over time. Although there is much scatter in the diffusion data, it is clear that the diffusion rates of oxygen in crystalline SiO_2 are slower than in amorphous SiO_2.[9] Crystallisation of some of the amorphous SiO_2 first formed on Si_3N_4 not only causes a progressive decrease of the cross-section area available for faster oxygen diffusion through the glass but also reduces the solubility and permeability of both oxygen and nitrogen. The effective O_2 diffusion coefficient in the oxide film decreases with an increasing amount of devitrified phases with time. Moreover, the presence of impurities in the intergranular phase causes an increase in the rate of crystallisation of silicon dioxide glasses and thus a decrease of the oxidation rate with time. Additionally, a reduction in nitrogen mobility in crystalline SiO_2 can lead to the formation of bubbles at the nitride/oxide interface because N_2 will not be able to diffuse out; if its pressure builds up cracking of a continuous crystalline SiO_2 layer may occur. Therefore, polyphase Si_3N_4 ceramics are very unlikely to follow simple oxidation rate laws because of the change in properties of the oxide layer with time. This approach to the analysis of oxidation kinetics highlights the need not only to consider multiple fitting models, but that changes of rate controlling mechanism with time will affect the mathematical fitting obtained. An incorrect fit will lead to the rate controlling mechanism being wrongly identified. Care must be taken because more than one single oxidation mechanism is most probably acting during oxidation making it difficult to predict long term behaviour. The fact that the oxidation process changes with time of exposure would render any data extrapolated beyond the maximum time actually tested potentially unreliable.

3.4 Oxide layers

The cross-sections of the oxide films formed on Ceranox NH209 after 50 h oxidation are shown in the micrographs in Figs 4 and 5. Owing to high atomic number contrast possible with backscattered electron (BSE), scale morphology, particularly with respect to Y, can readily be observed. The bright areas in the BSE images are attributed to high yttrium content. The identification of the crystalline oxidation products was established by a combination of XRD and energy dispersive analyses in the SEM.

The surface of the oxide layer was found to consist of four main components: a glassy phase, dark and light crystals embedded in the glass and pores. Preliminary microstructural studies of the oxide layers were carried out by SEM together with energy dispersive X-ray analysis (EDX) and XRD. At both 800 and 900°C, the oxide films are mostly amorphous (only traces of tridymite and yttrium silicates were identified by XRD), but as the oxidation

temperature was increased crystals were found to nucleate and grow preferably at the gas/oxide interface (as $Y_2Si_2O_7$) and at the nitride/scale interface (mainly SiO_2). EDX analyses revealed that the light crystals contained Y, Si and O and therefore correspond to the needle-like and/or plate-like yttrium silicates (Y_2SiO_5 and $Y_2Si_2O_7$) identified by XRD. The size and shape of these

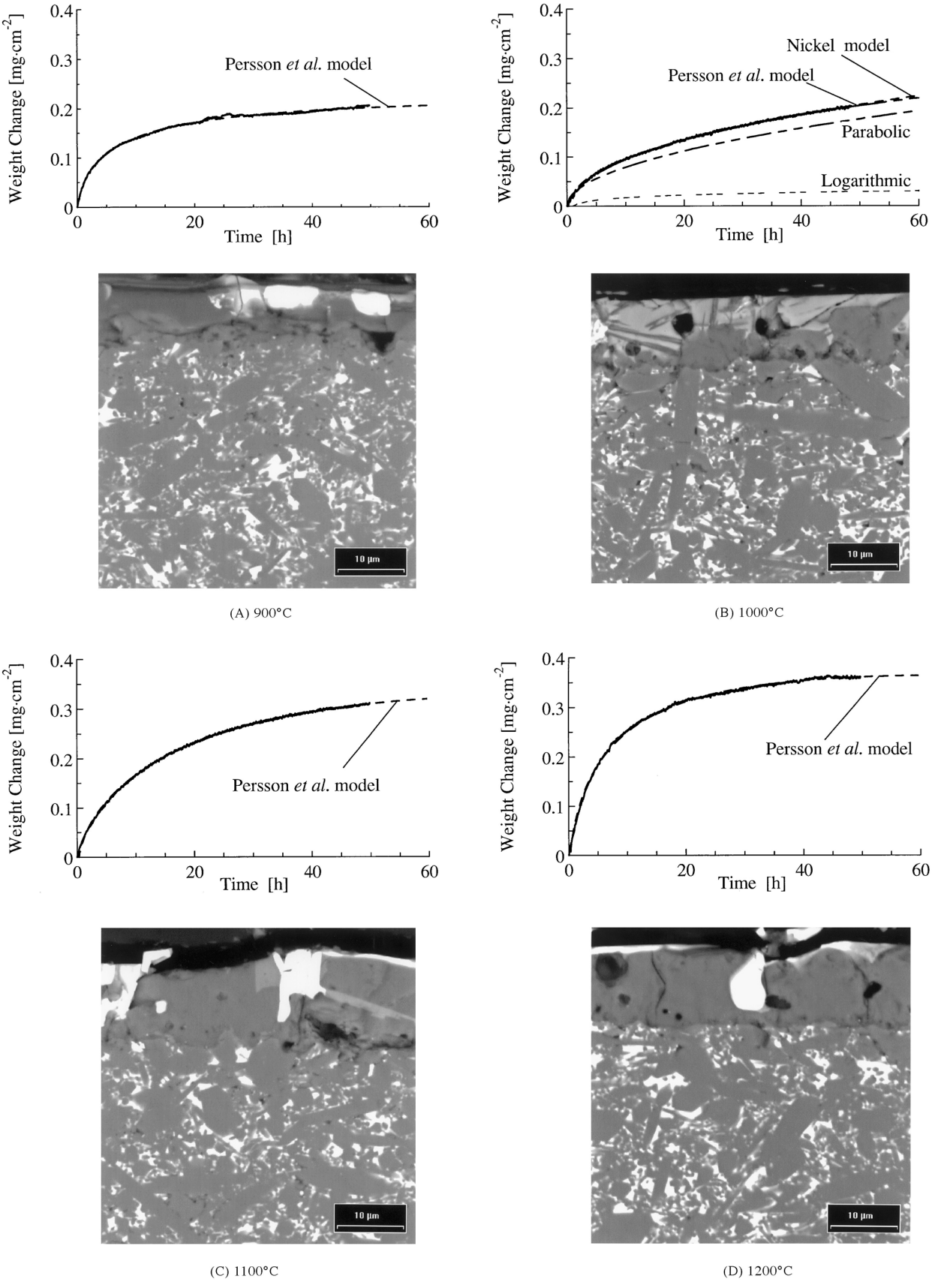

Fig. 5. Fitting of the kinetic data obtained at (a) 900°C (B), 1000°C (C), 1100°C (D) and 1200°C as well as BSE micrographs of a cross-section obtained after 50 h of exposure. (Note that in all micrographs the surface oxide film is shown at the top part of the images.)

crystals is temperature dependent. The dark crystals were found by EDX to contain Si and O and thus correspond to SiO_2 crystals (tridymite and cristobalite). In all cases, the glass phase was cracked, probably due mainly to the large volume change in the $\beta \rightarrow \alpha$ cristobalite phase transformation on cooling. Finally, some pores, associated with the inability of at least some N_2 to escape by diffusion through the silicate glass, were observed. A comparison of cristobalite content in samples oxidised at various temperatures showed that the degree of crystallinity of the surface layer increases with increasing oxidation temperature (this is also apparent in Figs 4 and 5). The existence of cristobalite (the crystalline form of SiO_2 which is stable above 1470°C[9]) at temperatures as low as 1000°C suggests that additive and impurity cations must play a role in its formation. The elements Y, Al, Fe, Mg, and Ca were detected by EDX in the glassy surface layer. Their presence, usually in ionic form (Y^{3+}, Fe^{3+}, Al^{3+}, Mg^{2+} and Ca^{2+}) not only reduce glass viscosity, thereby enhancing devitrification,[10] but also promote ionic mobility. Thus, it is evident that both the additives and impurities present in the material form mixed silicates like (Al, Mg, Ca, Fe)SiO_2 in addition to crystalline SiO_2 (both tridymite and cristobalite) as well as yttrium silicates mainly $Y_2Si_2O_7$ (note that Y_2SiO_5 crystals were only detected by XRD at 900°C).

4 Conclusions

It has been shown that the oxidation resistance depends on the formation of a protective SiO_2-rich layer but that exact composition and morphology of the layer are influenced by temperature of exposure. The exposure of the material below 1000°C did not result in catastrophic oxidation as observed for other Y_2O_3-doped hot pressed Si_3N_4 compositions. At 800°C, however, the occurrence of internal oxidation most likely takes place due to the formation of a non-protective oxide layer after the break-up of an initial protective film. At 900°C and above, as soon as an oxide layer completely covers the material's surface, its crystallisation with time (enhanced by the presence of the intergranular phase) leads to deviations from the parabolic rate law owing to reduced rates of diffusion through the crystalline material. This study has shown that the oxidation mechanism is complex and time of exposure dependent. As a consequence care must be taken in any mathematical modelling of oxidation kinetics. Only a close correlation of kinetic data and composition and morphological information can enable adequate characterisation of oxidation behaviour to be achieved.

Acknowledgements

One of the authors (FCO) wishes to thank the European Commission for a post-doctoral grant. The assistance provided by R. J. Fordham, P. Moretto, J. Van Eijk, P. Tambuyser, P. Frampton and K. Schuster is acknowledged. This work was carried out within the European Commission's Research and Development Programme.

References

1. Gazza, G. E., Hot-pressed Si_3N_4. *J. Am. Ceram. Soc*, 1973, **56**, 662.
2. Lange, F. F., Singhal, S. G. and Kuznicki, R. C., Phase relations and stability studies in the Si_3N_4–SiO_2–Y_2O_3 pseudoternary system. *J. Am. Ceram. Soc*, 1977, **60**, 249–252.
3. Patel, J. K. and Thompson, D. P., The low-temperature oxidation problem in yttria-densified silicon nitride ceramics. *Br. Ceram. Trans. J*, 1988, **87**, 70–73.
4. Persson, J., Käll, P. and Nygren, M., Interpretation of the parabolic and nonparabolic oxidation behavior of silicon oxynitride. *J. Am. Ceram. Soc*, 1992, **75**, 3377–3384.
5. Lange, F. F., Silicon nitride polyphase systems: fabrication, microstructure, and properties. *International Metals Reviews*, 1980, **25**, 1–20.
6. Wills, R. R., Cunningham, J. A., Wimmer, J. M. and Stewart, R. W., Stability of the silicon yttrium oxynitrides. *J. Am. Ceram. Soc*, 1976, **59**, 269–270.
7. Veyret, J. B., Comportement à l'oxydation de céramiques à base de nitrure de silicium en atmosphère complexe air/SO_2. PhD thesis, University of Limoges, France, 1989.
8. Nickel, K. G., Multiple law modelling for the oxidation of advanced ceramics and a model-independent figure of merit. In *Corrosion of Advanced Ceramics: Measurement and Modelling*, Vol. 267, ed. K. G. Nickel. NATO ASI Series E. Kluwer Academic, Dordrecht, The Netherlands, 1994, pp. 59-71.
9. Lamkin, M. A., Riley, F. L. and Fordham, R. J., Oxygen mobility in silicon dioxide and silicate glasses: a review.. *Journal of the European Ceramic Society*, 1992, **10**, 347–367.
10. Singhal, S. C., Thermodynamics and kinetics of oxidation of hot-pressed silicon nitride. *J. Mat. Sci.*, 1976, **11**, 500–509.